Supporting Information

Monitoring Neuroinflammation with an HOCl-Activatable and Blood−Brain Barrier Permeable Upconversion Nanoprobe

Meng Zhang[†], Miaomiao Zuo[‡], Caixia Wang[‡], Zhen Li[*,‡], Qingyuan Cheng[§], Ju Huang[†], Zijun Wang[†], Zhihong Liu[*,†,‡]

[†]College of Chemistry and Molecular Sciences, Wuhan University, Wuhan 430072, China

[‡] Ministry of Education Key Laboratory for the Synthesis and Application of Organic Functional Molecules and College of Chemistry and Chemical Engineering, Hubei University, Wuhan 430062, China

[§]Department of Clinical Laboratory, Zhongnan Hospital of Wuhan University, Wuhan, 430071, China.

*Corresponding author: Zhen Li; Zhihong Liu

Email: zhenli@whu.edu.cn; zhhliu@whu.edu.cn

Table of Contents

Materials. 1-Octadecene, oleic acid and glutathione were purchased from Aladdin Reagent, Ltd. (Shanghai, China). Lipopolysaccharide and minocycline were purchased from Sigma-Aldrich. DSPE-PEG_{2000} was acquired from Ponsure biological Co., Ltd. (Shanghai, China). ANG-DSPE-PEG_{2000} was obtained from Ruixi biological technology Co., Ltd. (Xi-an, China). Mouse IL-1 beta uncoated ELISA Kit was purchased from Thermo Fisher (USA). Mouse myeloperoxidase (MPO) ELISA Kit was obtained from NeoBiscience (USA). Other chemical reagents were purchased from Sinopharm Chemical Reagent Co., Ltd. (Shanghai, China). All the reagents were analytical or better grade and used without further purification. All aqueous solution was prepared with ultrapure water (Mill-Q, Millipore, 18.2 MΩ·cm resistivity). Mice were supplied by Wuhan Centers for Disease Prevention & Control (Wuhan, China). All animal studies were performed in accordance with Animal Care and Use Committee of Wuhan University.

Instrumentation. The size and morphology of upconversion nanoparticles were characterized by the JEM-2010 transmission electron microscope (TEM) operated at 200 kV. XRD measurement was acquired by an X-ray diffractometer (XRD, Bruker D8 Discover) with a 2θ range of 10° - 80° with Cu Kα irradiation (k=1.5406 Å). FT-IR spectra were conducted on Nicolet 5700 FTIR Spectrometer (Thermo Fisher Scientific, USA). UV-Vis spectra were measured by UV 2550 UV-Vis spectrophotometer (Shimadzu, Japan). The UCL spectra were recorded on RF-6000 fluorophotometer

(Shimadzu, Japan) equipped with an external 980 nm CW laser (Beijing Hi-Tech Optoelectronic Co., Ltd.). CCK8 test was conducted on Mk3 microplate reader (Thermo Scientific Multiskan, USA). *In vivo* UCL imaging was acquired by PerkinElmer IVIS Spectrum. Gd content in the major organs of mice was analyzed by ICP-MS (PlasmaQuant MS, German). Gd content in *in vitro* BBB model was analyzed by ICP-OES (Thermo IRIS Intrepid II, USA).

Preparation of HOCl. The HOCl solution was prepared by diluting the commercial sodium hypochlorite solution with ultrapure water.[1] The concentration was determined by the UV-Vis absorbance at 292 nm. (ε=360 M^{-1} cm^{-1})

Preparation of $OONO^-$ solution. The $OONO^-$ solution was obtained by mixing of sodium nitrite solution (0.6 M, 3 mL), sodium hydroxide solution (1.5 M, 3 mL) and hydrogen peroxide (0.7 M, 1.5 mL) in hydrochloric acid (0.6 M, 1.5 mL).[2] Furthermore, the concentration of the $OONO^-$ solution was determined by measuring the UV-vis absorbance at 302 nm in 0.1 M NaOH. (ε=1670 M^{-1} cm^{-1})

Preparation of $O_2^{\bullet-}$ solution. Potassium superoxide (KO_2) was dissolved in DMSO under the condition of ultrasonication.[2] The concentration of $O_2^{\bullet-}$ was determined by measuring the UV-vis absorbance at 256 nm in 1 mM NaOH. (ε=2686 M^{-1} cm^{-1})

Preparation of •OH. •OH was prepared by fenton reaction between Iron(II) sulfate ($FeSO_4$) and hydrogen peroxide (H_2O_2).[2] Generally, $FeSO_4$ and H_2O_2 was respectively dissolved in dilute sulphuric acid with the final concentration of 0.1 mM and mixed them with the concentration ratio of 1:6.

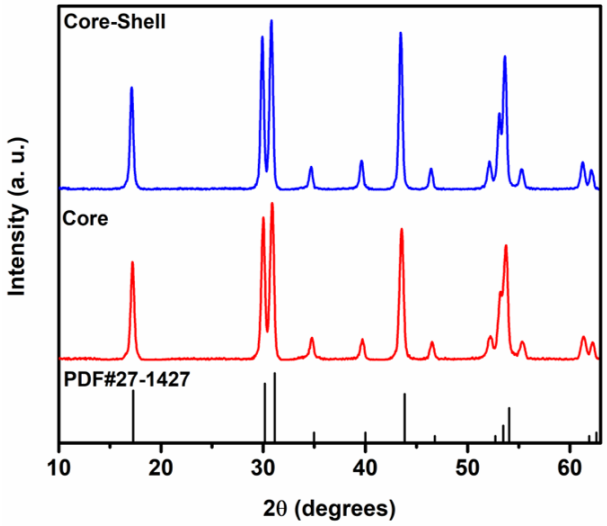

Figure S1. XRD patterns of the core nanoparticles $NaYbF_4$:0.25Gd, core−shell nanoparticles $NaYbF_4$:0.25Gd@$NaYF_4$:0.04Yb,0.015Tm, and the standard hexagonal $NaYbF_4$ crystal (Joint Committee on Powder Diffraction Standards file number 27-1427).

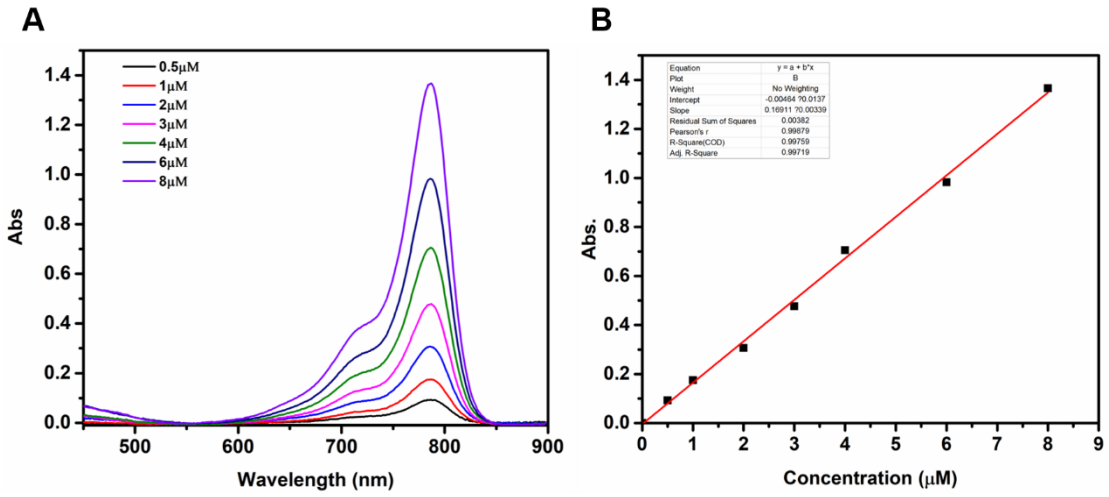

Figure S2. (A) UV-vis absorption spectra of **Cy-HOCl** in DMSO. (B) Linear relationship between UV-vis absorbance and the concentration of **Cy-HOCl** at 786 nm.

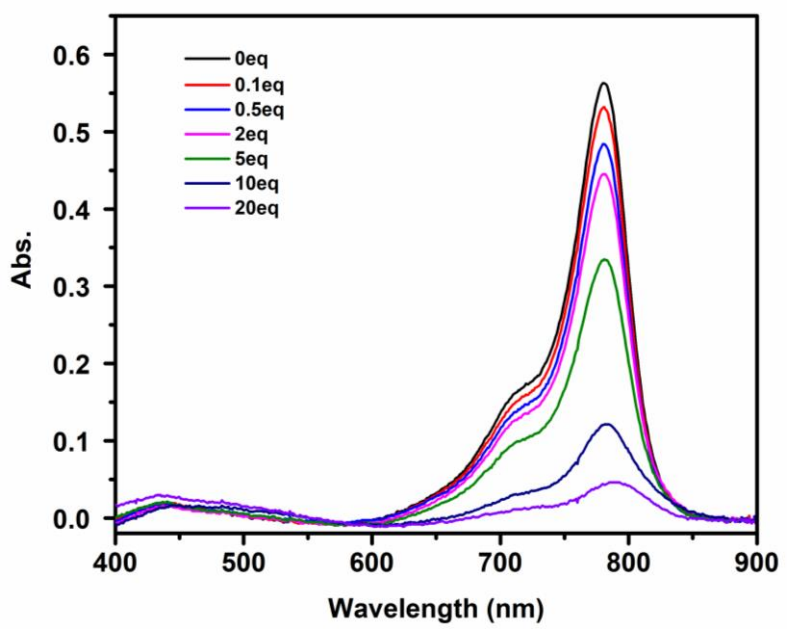

Figure S3. UV-vis absorption spectra of 10 μM **Cy-HOCl** after reacting with different equivalents of HOCl in the mixture solvent of DMF and boric acid buffer (v:v=1:1, pH=7.4, 20 mM).

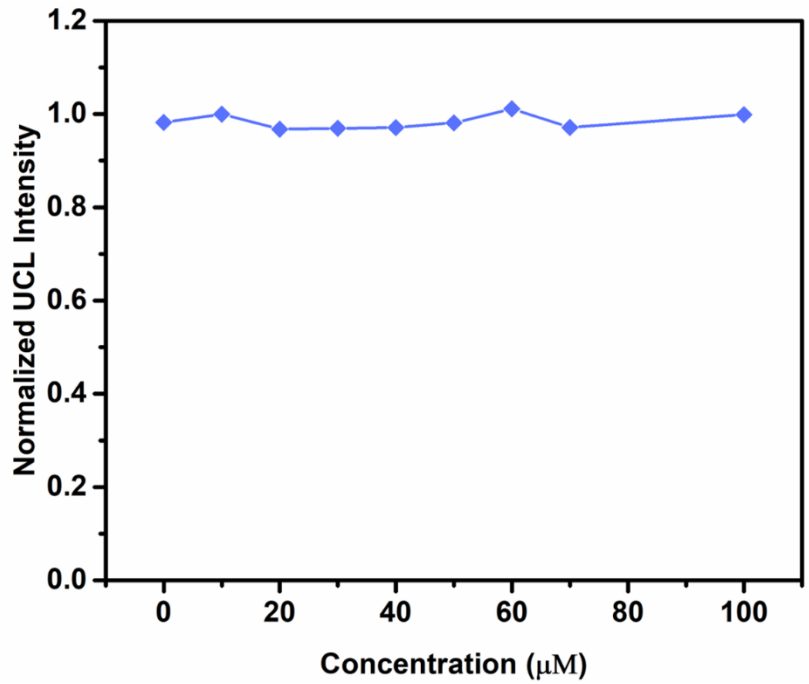

Figure S4. The UCL intensities of ANG-UCNPs after incubation with different concentrations of HOCl at 37 °C for 1 h in boric acid buffer (pH=7.4, 20 mM).

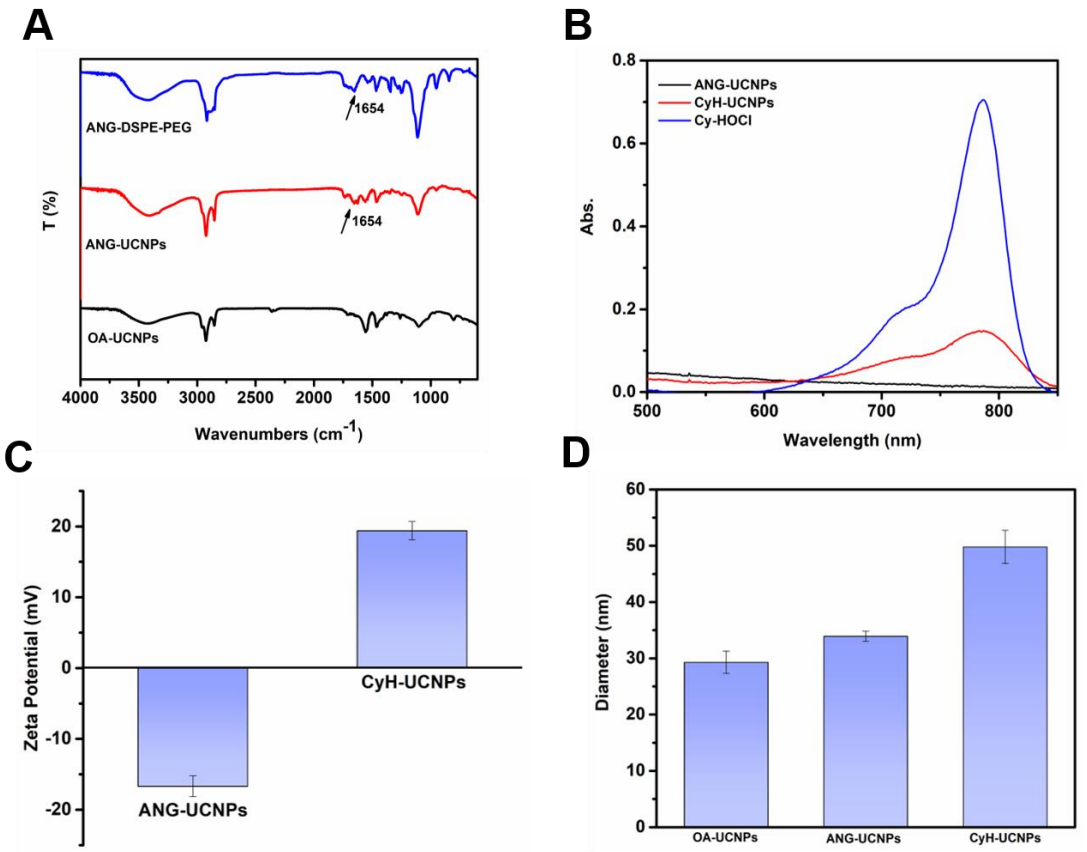

Figure S5. (A) FTIR spectra of OA-UCNPs, ANG-UCNPs, and ANG-DSPE-PEG. (B) UV−vis absorption spectra of **Cy-HOCl**, CyH-UCNPs, and ANG-UCNPs. (C) Zeta potentials of ANG-UCNPs and CyH-UCNPs. (D) The change of diameter of OA-UNPs, ANG-UCNPs, and CyH-UCNPs (note: the diameter of OA-UNPs was acquired by TEM images, the diameter of ANG-UCNPs and CyH-UCNPs were measured by DLS).

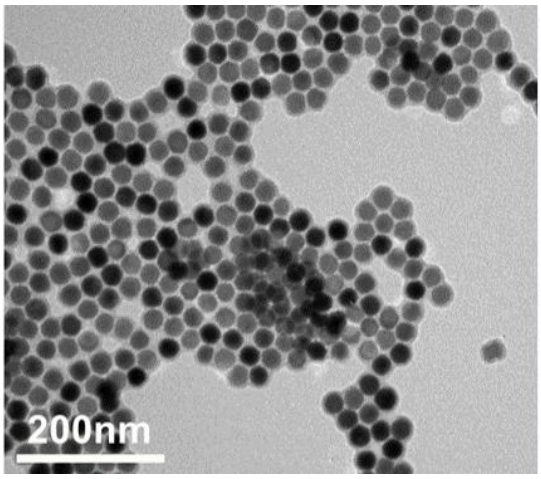

Figure S6. TEM image of CyH-UCNPs.

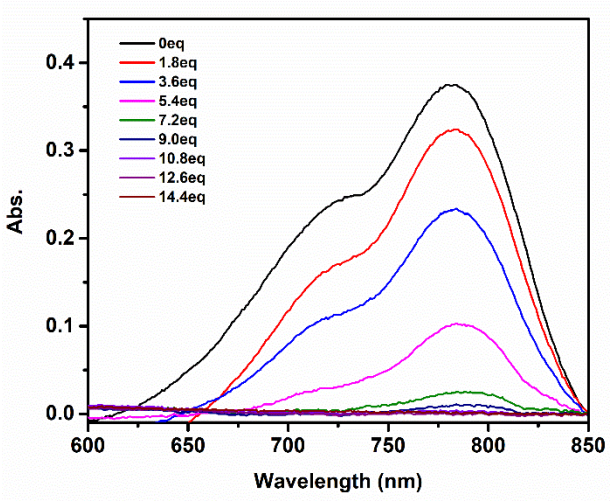

Figure S7. UV-vis absorption spectra of 2.17 μM **Cy-HOCl** assembled on the UCNPs after reacting with different equivalents of HOCl in boric acid buffer (pH=7.4, 20 mM).

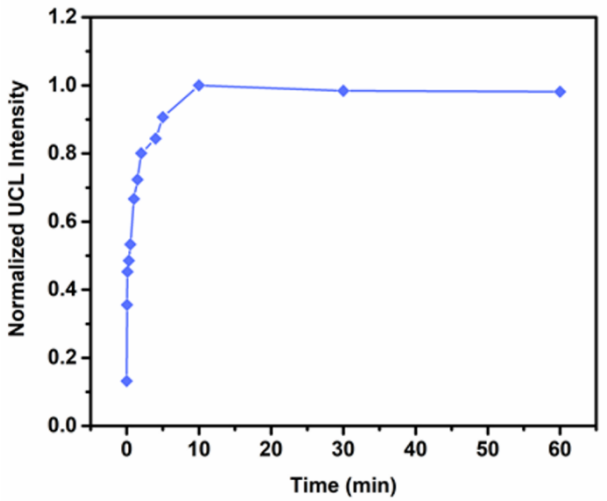

Figure S8. Dependence of the UCL intensity at 800 nm of CyH-UCNPs on the time of reaction with 10 μM HOCl at 37°C in boric acid buffer (pH=7.4, 20 mM).

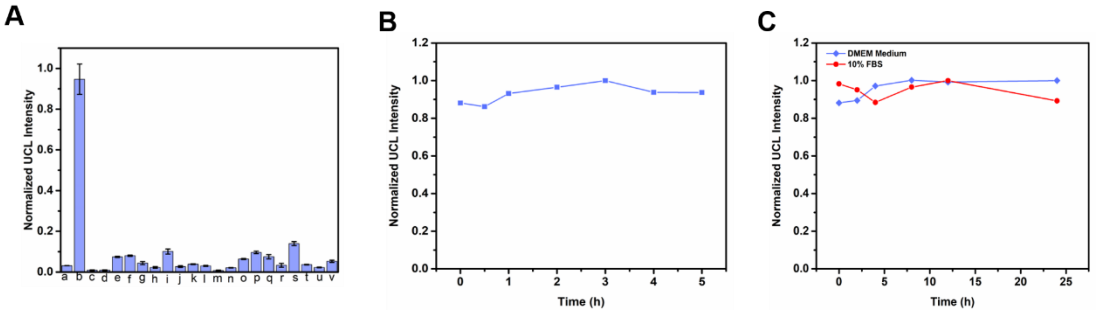

Figure S9. (A) Response of CyH-UCNPs to the potential interferents and HOCl. (a: blank, b: 20 μM HOCl, c,d: Cu^{2+}, Fe^{3+} (200 μM), e-i: Ca^{2+}, Mn^{2+}, Li^{3+}, Mg^{2+}, Zn^{2+} (1 mM), j,k: K^{+}, Na^{+} (10 mM), l-q: Hcy, Lys, His, Na_2S, GSH, H_2O_2 (1 mM), r: $O_2^{\cdot-}$ (200 μM), s,t: $ONOO^{-}$, ·OH (100 μM), u: BSA (0.1 mg/mL), v: glucose (1 mM)). (B) Thermal stability of CyH-UCNPs (0.05 mg/mL) in boric acid buffer (pH=7.4, 20 mM) at 37°C. (C) Stability of CyH-UCNPs (0.05 mg/mL) in the different media at 37°C.

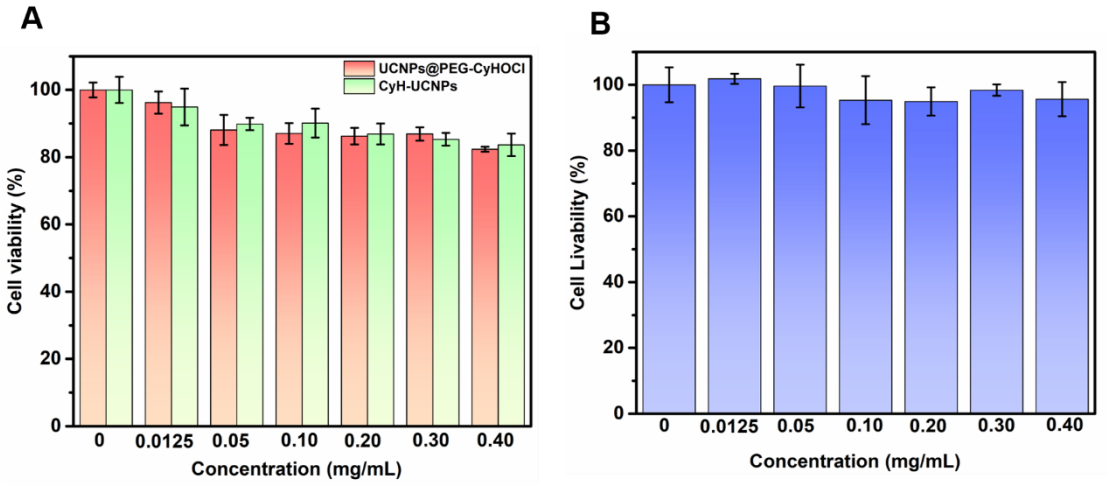

Figure S10. (A) The viability of human brain microvascular endothelial cell after incubation with different concentrations of CyH-UCNPs and UCNPs@PEG-CyHOCl for 24 h. (B) The viability of PC12 cell after incubation with different concentrations of CyH-UCNPs for 24 h.

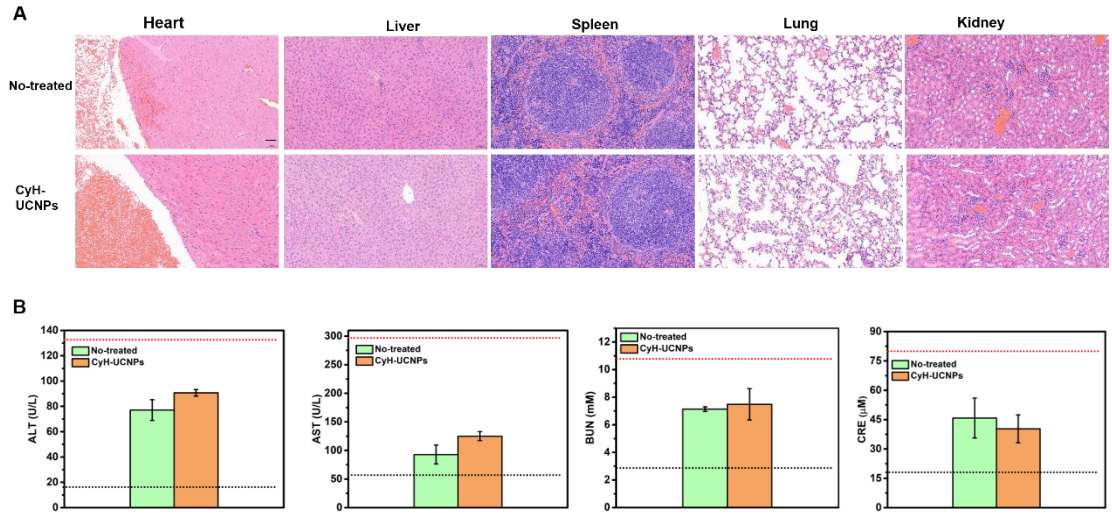

Figure S11. (A) H&E staining assays of the mice major organs with or without CyH-UCNPs treatment for 7 days. Scale bar: 50 μm. (B) Blood biochemical analysis of the mice with or without CyH-UCNPs treatment for 7 days. The red and black lines represent the highest and lowest reference value of alanine aminotransferase (ALT), aspartate aminotransferase (AST), blood urea nitrogen (BUN) and creatinine (CRE), respectively.[3]

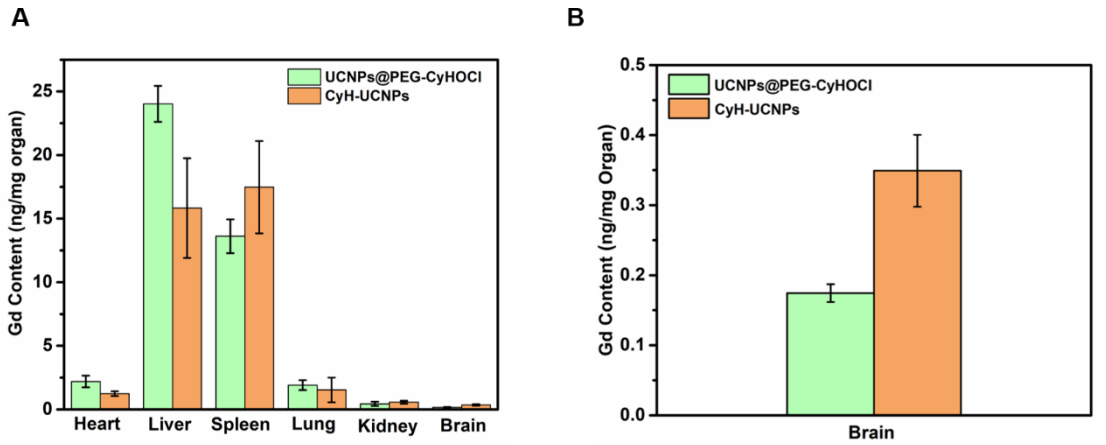

Figure S12. (A) The biodistribution of CyH-UCNPs and UCNPs@PEG-CyHOCl in the major organs of healthy mice after i.v. injection for 4 h by analyzing Gd content using ICP-MS. (B) The biodistributions of UCNPs@PEG-CyHOCl and CyH-UCNPs in the brain of healthy mice after i.v. injection for 4 h by analyzing Gd content using ICP-MS.

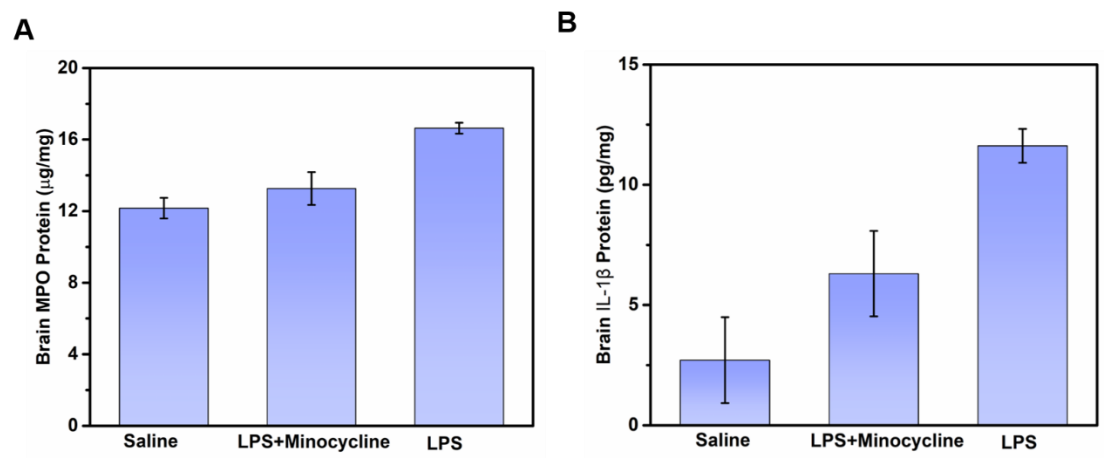

Figure S13. The expression levels of inflammation-related protein MPO (A) and pro-inflammatory cytokines IL-1β (B) in the brain tissue of the mice with different treatments.

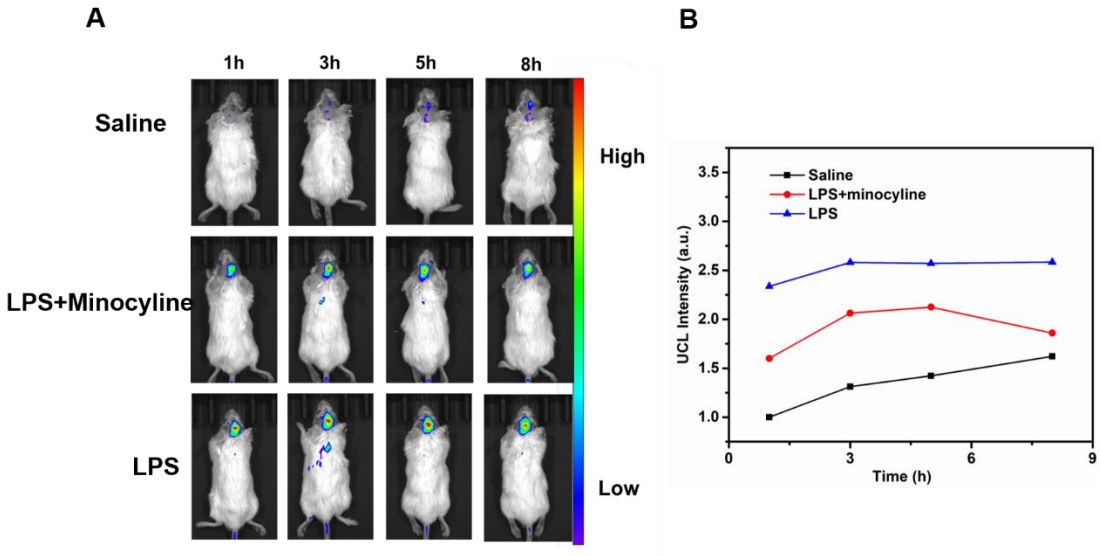

Figure S14. (A) *In vivo* UCL imaging of the mice with different treatments at 1, 3, 5, and 8 h after intravenous injection with CyH-UCNPs. (B) UCL intensities in images (A).

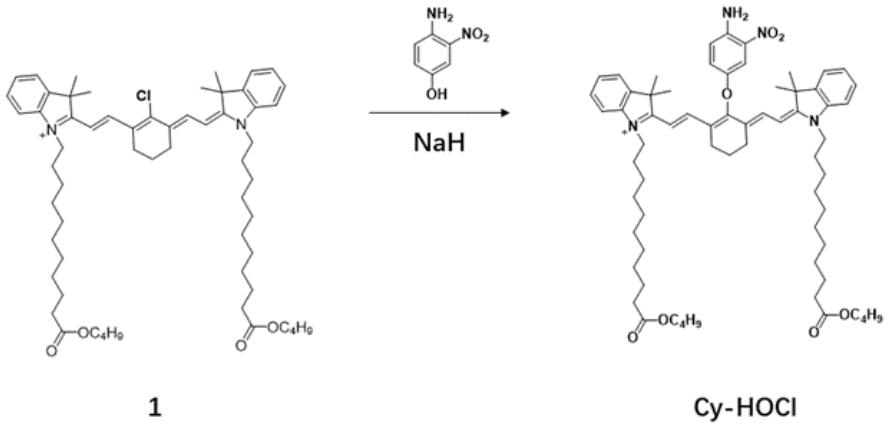

Figure S15. Synthetic routine of **Cy-HOCl**.

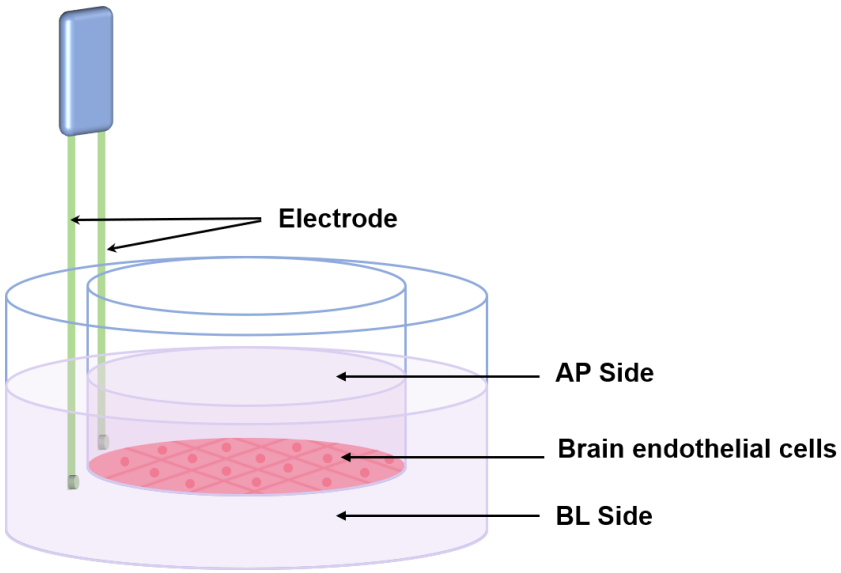

Figure S16. Schematic illustration of the measurement of TEER value.

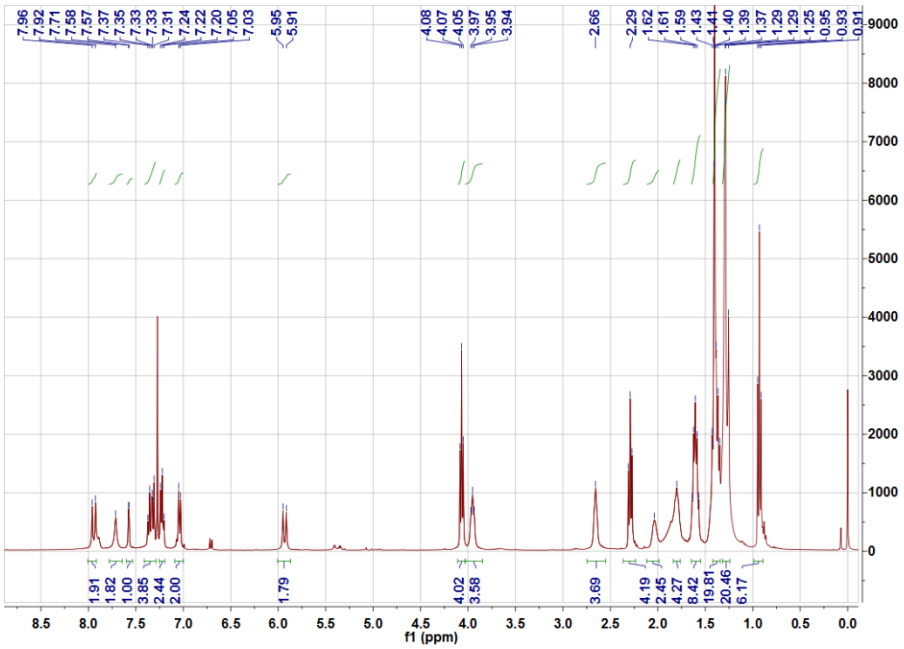

Figure S17. ^{1}H NMR spectrum of **Cy-HOCl**.

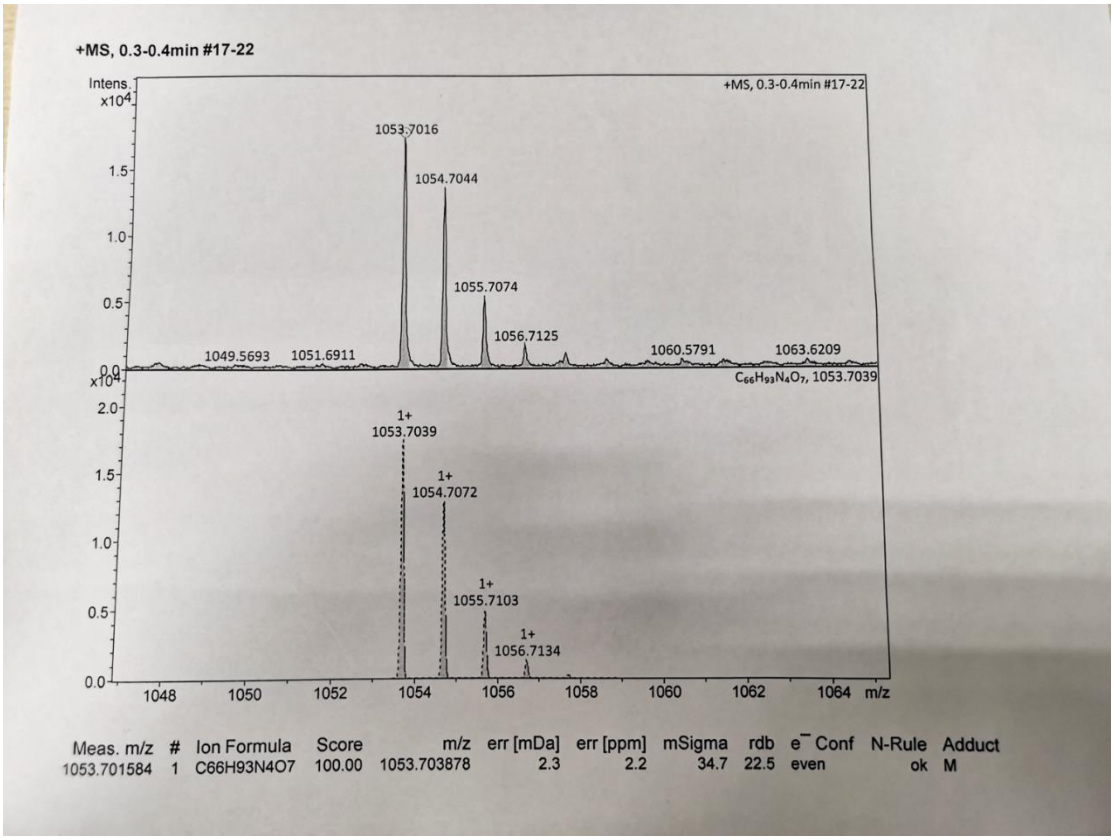

Figure S18. High resolution mass spectrum (HRMS) of **Cy-HOCl**.

Reference

[1] Zeng, L.; Xia, T.; Hu, W.; Chen, S.; Chi, S.; Lei, Y.; Liu, Z. *Anal. Chem.* **2018**, *90*, 1317−1324.

[2] Ai, X.; Wang, Z.; Cheong, H.; Wang, Y.; Zhang, R.; Lin, J.; Zheng, Y.; Gao, M.; Xing, B. *Nat. Commun.* **2019**, *10*, 1087.

[3] Gong, N.; Ma, X.; Ye, X.; Zhou, Q.; Chen, X.; Tan, X. *Nat. Nanotech.* **2019**, *14*, 379–387.